Crystal Water Dynamics of Guanosine Dihydrate: Analysis of Atomic Displacement Parameters, Time Profile of Hydrogen-Bonding Probability, and Translocation of Water by MD Simulation

Shigetaka Yoneda,*,† Yoko Sugawara,† and Hisako Urabe‡

School of Science, Kitasato University, Kitasato, Sagamihara, Kanagawa 228-8555, Japan, and Tokyo Kasei Gakuin University, Aihara, Machida, Tokyo 194-0292, Japan

Received: August 19, 2004

The dynamics of crystal water molecules of guanosine dihydrate are investigated in detail by molecular dynamics (MD) simulation. A 2 ns simulation is performed using a periodic boundary box composed of 4 × 5 × 8 crystallographic unit cells and using the particle-mesh Ewald method for calculation of electrostatic energy. The simulated average atomic positions and atomic displacement parameters are remarkably coincident with the experimental values determined by X-ray analysis, confirming the high accuracy of this simulation. The dynamics of crystal water are analyzed in terms of atomic displacement parameters, orientation vectors, order parameters, self-correlation functions of the orientation vectors, time profiles of hydrogen-bonding probability, and translocations. The simulation clarifies that the average structure is composed of various stable and transient structures of the molecules. The simulated guanosine crystal forms a layered structure, with four water sites per asymmetric unit, classified as either interlayer water or intralayer water. From a detailed analysis of the translocations of water molecules in the simulation, columns of intralayer water molecules along the *c* axis appear to represent a pathway for hydration and dehydration by a kind of molecular valve mechanism.

Introduction

Water molecules are common components of biomolecular crystals. For example, protein crystals contain 30−70% v/v water, and even crystals of small molecules such as vitamin B_{12} contain 10−20% w/w water. Many nucleoside and nucleotide crystals contain 10−30% w/w water, where the water exists between the molecular layers, and these crystals have been shown to exhibit humidity-dependent phase transitions. These transitions were first discovered by gravimetric measurements,[1] and subsequent X-ray, Raman spectroscopy, and high-resolution solid-state nuclear magnetic resonance (NMR) analyses have revealed the transitions of sodium salts of inosine 5′-phosphate,[2−5] disodium adenosine 5′-triphosphate (Na_2·ATP),[6−8] guanosine,[7,9] and disodium cytidine 5′-monophosphate (Na_2·CMP).[10] The characteristics of the humidity-dependent phase transitions of hydrates are of interest because of the implications for the pseudopolymorphism of medical drugs, with importance for the pharmaceutical industry. Analysis of the mechanisms of humidity-dependent phase transitions is also of interest in the study of organic crystal dynamics and has provided sharp insights into the hydrophobic interaction of nucleic acids in biological environments.

Humidity-induced phase transitions are triggered by a change in the number of crystal water molecules. Therefore, the dynamics of crystal water is an important aspect of analysis of the hydrates. Although the macroscopic behavior of crystal components can be described by spectroscopic study of dielectric dispersions, it is difficult to discuss the character of individual crystal water molecules by this approach. Crystallographic analysis is limited in that it is difficult to distinguish whether the observed structural disorder is static or dynamic. Molecular dynamics (MD) simulation is an effective method for obtaining complimentary information, and provides a means for a comprehensive analysis.

Of the many nucleotides and nucleosides, guanosine has been studied extensively with respect to its structural transition. Guanosine crystallizes from an aqueous solution as a dihydrate[11] with space group $P2_1$, consisting of two guanosine molecules, GA and GB, and four water molecules, W1−W4, in an asymmetric unit, as shown in Figure 1. The guanine bases of GA and GB are stacked alternately along the *c* axis, and are hydrogen bonded along the *b* axis to form molecular layers. Water molecules W1 and W2 are located in the cavity of the molecular layers of guanosine and are stacked along the *c* axis to form a column. This configuration is called intralayer water.[7,9] Water molecules W3 and W4 are located between two molecular layers as interlayer water, bridging two molecular layers of guanosine by hydrogen bonds. The interlayer water does not form a clear column in the crystal.

The hydration number of a guanosine molecule changes reversibly from 2 (H state) to 0 (A state) over a relative humidity range of 0−20%, with some hysteresis. In the dehydration process, the hydration number remains at 2 until the relative humidity decreases to around 10%. In contrast, in the hydration process beginning from the A state, the hydration number reverts to 2 at around 20% relative humidity, passing through an intermediate state of 1.3 hydrate (M state), which is stable at 10−20% relative humidity. Judging from the change in the cell constants, the escape of intralayer water molecules from the crystals precedes the escape of interlayer water in the dehydration process. However, the intralayer water sites become

* Corresponding author. Phone: +81 42 778 9404. Fax: +81 42 778 9538. E-mail: yoneda@sci.kitasato-u.ac.jp.
† Kitasato University.
‡ Tokyo Kasei Gakuin University.

10.1021/jp046258j CCC: $30.25
Published on Web 12/31/2004

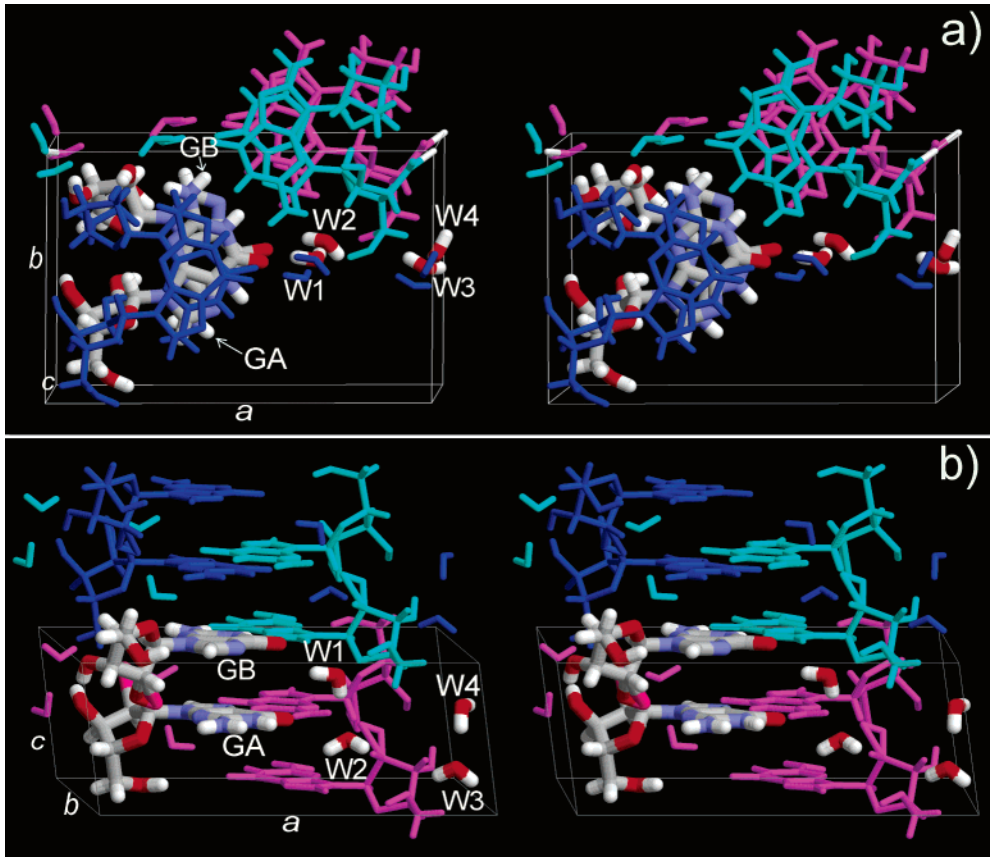

Figure 1. X-ray structure of a guanosine dihydrate crystal viewed (a) along the *c* axis and (b) obliquely.

populated by water molecules before the interlayer water sites in the hydration process (i.e., the M state). This behavior indicates that the structural transition of guanosine crystal is under kinetic or dynamic control, as water molecules with weaker equilibration constants would escape early and bind late if the transition was governed by equilibrium thermodynamics. The dynamics of the intralayer and interlayer water molecules in guanosine dihydrate was examined in detail in this study through MD simulations, and the hydration−dehydration pathway will be discussed.

Theoretical Calculations

A 2 ns MD simulation of guanosine dihydrate crystal was performed using the AMBER 6 program[12] with periodic boundary conditions. The cell parameters of guanosine dihydrate were as follows: $a = 17.518(3)$ Å, $b = 11.502(1)$ Å, $c = 6.658(1)$ Å, and $\beta = 98.17°$ (the numbers in parentheses denote experimental standard error).[11] The crystallographic unit cell was replicated $4 \times 5 \times 8$ times in the *a*, *b*, and *c* directions, respectively, to form initial coordinates. Thus, the periodic boundary box was a parallelepiped with side lengths of 70.072, 57.510, and 53.264 Å and contained 160 unit cells, 320 asymmetric units, 640 guanosine molecules, 1280 water molecules, and 24 960 atoms. MD simulations were performed after energy minimization of the initial structure. Figure 2 shows a snapshot of the periodic boundary box at 2 ns. The *x* and *y* axes of the Cartesian coordinates adopted for the MD simulation are aligned parallel to the *a* and *b* axes, respectively. The *c* axis is declined with respect to the *z* axis by 8.17°. AMBER ff99 energy parameters[13] and TIP3P water parameters[14] were used for the simulation. Electrostatic interactions were calculated by the particle-mesh Ewald method[15] using a real-space cutoff distance of 8 Å, an Ewald screening parameter of 0.348 64 $Å^{-1}$, a grid density of ~ 1 $Å^{-1}$ for fast Fourier transformation, and a fourth-order spline function for interpolation between grid nodes. No positional constraints were applied. The size and volume of the periodic boundary box were fixed. A time step of 0.5 fs was adopted, and the leapfrog integration method was used. Net translation and rotation of the system were removed every 100 steps. The initial temperature was set at 100 K, and the temperature was maintained at 300 K by scaling the velocity[16] with a relaxation time of 10 ps in the first 40 ps of simulation and 1 ps thereafter. The coordinates were stored at 0.05 ps intervals for analysis.

The calculation of root-mean-square deviations (rmsd's) is not straightforward for water molecules in the present system because the water molecules translocate in the crystal. The X-ray positions of water molecules are designated as water sites S1−S4, corresponding to the sites initially occupied by W1−W4, respectively. A water molecule is judged to have translocated when the distance of the water oxygen atom from its initial site is no shorter than the distances to any other site. When there is no water oxygen atom within a distance criterion, R_e, from a water site, the site is considered to be empty. When one or two water oxygen atoms are present within distance R_e, the site is defined to be singly or doubly occupied. An R_e value of 2.2 Å was adopted in the present simulations. For calculations of rmsd's, the coordinates of the site closest to each water molecule were used as reference coordinates for the water molecule. As the positions of the two hydrogen atoms, H1 and H2, of the water molecules were often exchanged due to rotation of the water molecule, the hydrogen atom closest to the X-ray position of H1 was designated H1 and the other hydrogen atom was designated H2.

The rms fluctuations of atoms were calculated by the above procedure for rmsd and then transformed into Debye−Waller

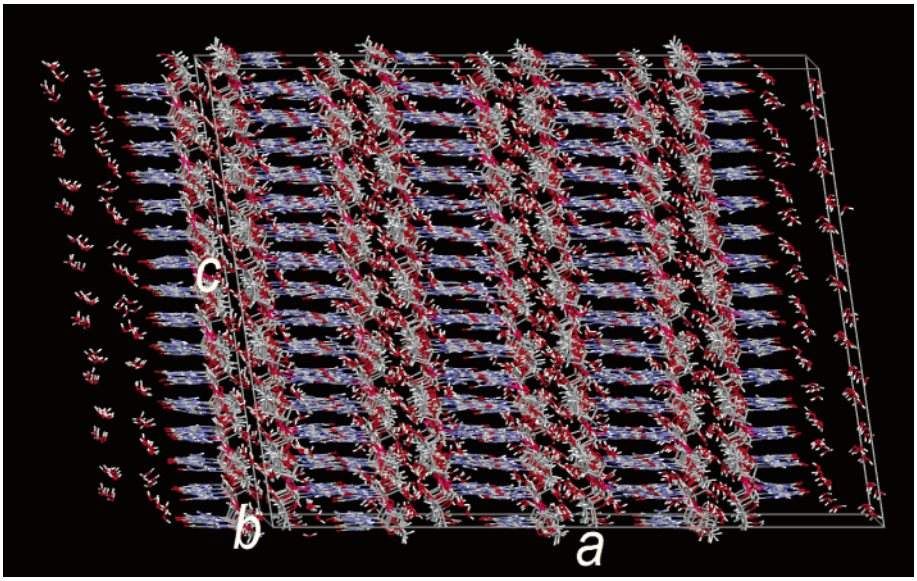

Figure 2. Snapshot at 2 ns.

atomic displacement parameters (*B*-factors) using the following formula: $B = (8\pi^2/3)\langle(\Delta x_i)^2 + (\Delta y_i)^2 + (\Delta z_i)^2\rangle$, where Δx_i, Δy_i, and Δz_i are the instantaneous displacements of atom *i* from the average position in the *x*, *y*, and *z* directions and $\langle ... \rangle$ denotes the average.[17] The average was calculated between 1 and 2 ns for all 320 asymmetric units. The data for water molecules located at a current water site were accumulated for calculation of the *B*-factors of the site. The directional components of the temperature factors, $B_x = (8\pi^2/3)\langle(\Delta x_i)^2\rangle$, $B_y = (8\pi^2/3)\langle(\Delta y_i)^2\rangle$, and $B_z = (8\pi^2/3)\langle(\Delta z_i)^2\rangle$, were also calculated.

The unit cell in the periodic boundary box is represented by (i_x, i_y, i_z), where $i_x = 0-3$, $i_y = 0-4$, and $i_z = 0-7$. The coordinates x', y', and z' of an atom in the unit cell (i_x, i_y, i_z) are related to the coordinates *x*, *y*, and *z* of the corresponding atom in the unit cell (0, 0, 0) as follows: $x' = x + ai_x + c(\cos\beta)i_z$, $y' = y + bi_y$, and $z' = z + c(\sin\beta)i_z$. Similarly, each asymmetric unit is denoted by (i_{as}, i_x, i_y, i_z), and the coordinates x', y', and z' in the asymmetric unit (1, 0, 0, 0) are related to the coordinates *x*, *y*, and *z* in the asymmetric unit (0, 0, 0, 0) as follows: $x' = -x + c(\cos\beta)$, $y' = y + b/2$, and $z' = -z + c(\sin\beta)$. For example, the white parallelepiped in Figure 1 is a unit cell composed of two asymmetric units, (0, 0, 0, 0) and (1, 1, 0, 0). The atoms in CPK colors (the colors adopted for the CPK models), magenta, blue, and cyan belong to (0, 0, 0, 0), (1, 1, 0, 0), (0, 0, 0, 1), and (1, 1, 0, 1), respectively. An atom is denoted by (i_{at}, i_m, i_{as}, i_x, i_y, i_z), where i_{at} and i_m are the atom name and molecule name, respectively. As water molecules translocate in this simulation, water molecules are identified in terms of initial X-ray positions in the form (i_m, i_{as}, i_x, i_y, i_z).

For analysis of the orientation of water molecules, two unit vectors, $\mathbf{v}_b$ and $\mathbf{v}_n$, were defined, where $\mathbf{v}_b$ is the bisector between the oxygen atom and the two hydrogen atoms showing the reverse direction of the dipole moment of water and $\mathbf{v}_n$ is the vector orthogonal to the plane defined by the oxygen atom and the two hydrogen atoms. As the two asymmetric units are related by a 2-fold axis (i.e., 180° rotation), the directions of the average vectors are antiparallel to each other in asymmetric units with i_{as} values of 0 and 1: The average of the vectors for water molecules is represented in the asymmetric unit with an i_{as} value of 0. Fluctuations of $\mathbf{v}_b$ and $\mathbf{v}_n$ were transformed into the molecular-order parameter, *S*, using the formula $S = (1/2)(3\langle\cos^2\theta\rangle - 1)$, where θ is the instantaneous angle from the averaged direction[18] and $\langle ... \rangle$ is the average over all asymmetric units for the period from 1 to 2 ns. The calculation of $\mathbf{v}_n$ is not straightforward because $\mathbf{v}_n$ and its inverse vector $-\mathbf{v}_n$ give the same orientation of the water molecule. Thus, to average $\mathbf{v}_n$, it is first necessary to calculate the averages of the products of $\mathbf{v}_{n,i}$ and $\mathbf{v}_{n,j}$, denoted $\langle\mathbf{v}_{n,i}\mathbf{v}_{n,j}\rangle$, where *i* and *j* equal 1, 2, or 3, corresponding to the *x*, *y*, or *z* directions, respectively. The eigenvectors of the matrix are then calculated for $\langle\mathbf{v}_{n,i}\mathbf{v}_{n,j}\rangle$, using the eigenvector of the largest eigenvalue for the averaged direction, $\langle\mathbf{v}_n\rangle$. The value of θ in $\langle\cos^2\theta\rangle$ of $\mathbf{v}_n$ was determined by calculating the difference from the averaged direction, and the $\langle\cos^2\theta\rangle$ thus determined was identical to the largest eigenvalue of $\langle\mathbf{v}_{n,i}\mathbf{v}_{n,j}\rangle$. The self-correlation functions of the orientation vectors, $\langle\mathbf{v}_b(t)\cdot\mathbf{v}_b(t+\Delta t)\rangle$ and $\langle|\mathbf{v}_n(t)\cdot\mathbf{v}_n(t+\Delta t)|\rangle$, were calculated by tracing the changes of the orientation vectors of each water molecule. The traced change was averaged over all asymmetric units and for *t* from 1.8 to 2.0 ns. The values of $\langle\mathbf{v}_b(t)\cdot\mathbf{v}_b(t+\Delta t)\rangle$ and $\langle|\mathbf{v}_n(t)\cdot\mathbf{v}_n(t+\Delta t)|\rangle$ should converge to $\langle\cos^2\theta\rangle$ of $\mathbf{v}_b$ and $\mathbf{v}_n$, respectively, when Δt is sufficiently large. The translocation of water was considered in the calculation of $\mathbf{v}_b$ and $\mathbf{v}_n$.

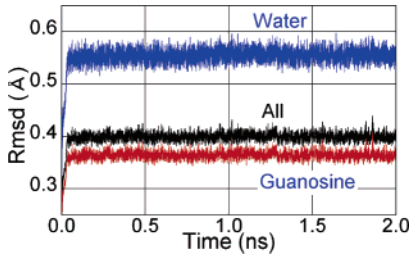

Figure 3. Time profile of rmsd from initial X-ray structure.

The criterion for hydrogen bonding adopted in this study is a donor−acceptor distance of <3.2 Å and a hydrogen−donor−acceptor angle of <30°. The 2 ns trajectory of the MD simulation was divided into 40 periods of 50 ps each, with each period representing 1000 structures. The hydrogen-bonding probability, P_{hb}, was determined by averaging N_{hb} over all 320 asymmetric units and 1000 structures, where N_{hb} is the number of pairs that satisfy the criterion. The translocation of water was not considered in the calculation of P_{hb}. The notation H21, H22, H5′, and H5″ for guanosine follows the IUPAC recommendation.[19] Water molecules W1, W2, W3, and W4 correspond to O11, O10, O13, and O12 by Thewalt,[11] respectively.

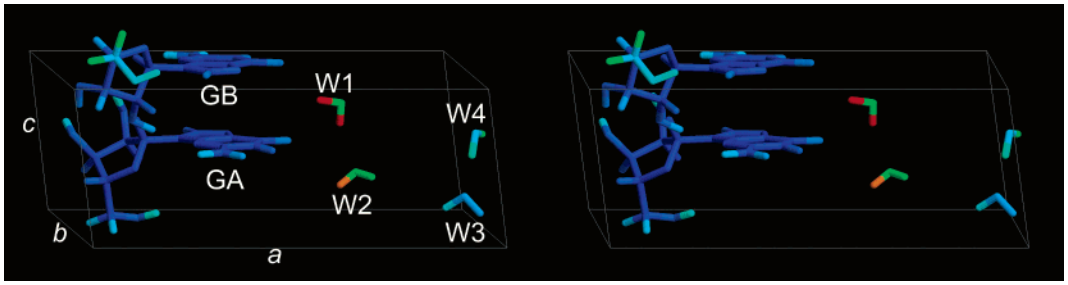

Figure 4. Averaged structure of asymmetric unit. The color gradient is based on the atomic fluctuations in Figure 6.

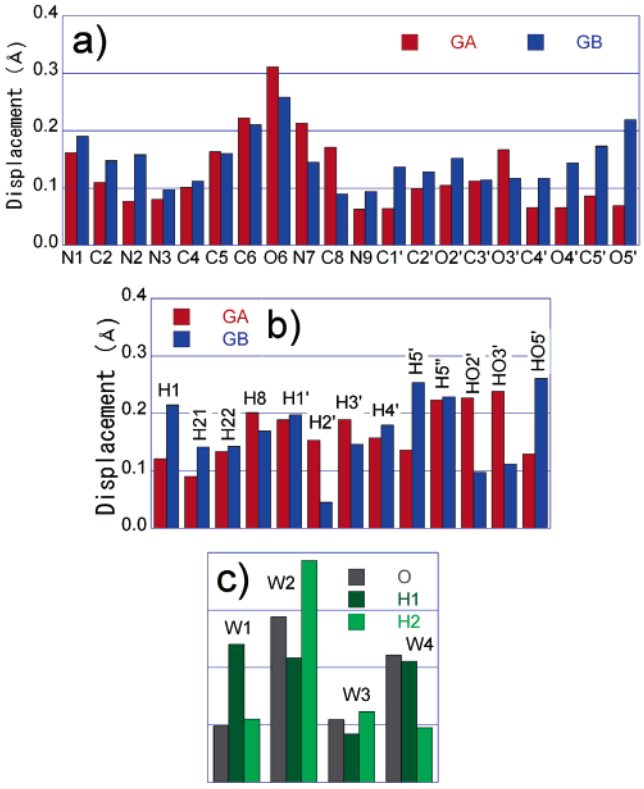

Figure 5. Displacement of average structure from the X-ray structure for (a) non-hydrogen atoms of guanosine, (b) hydrogen atoms of guanosine, and (c) all atoms of water.

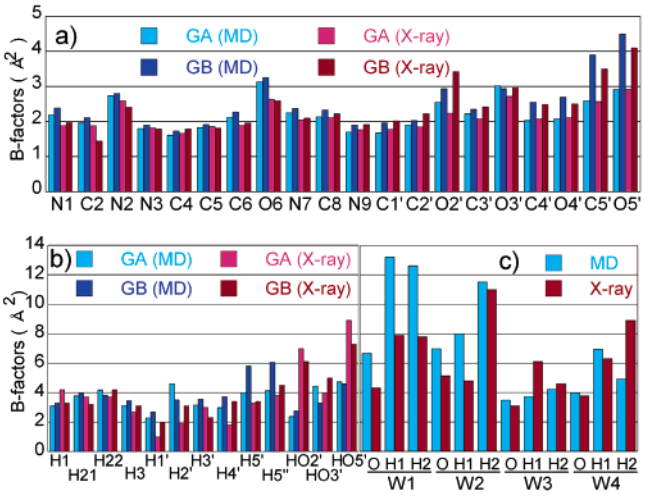

Figure 6. *B*-Factors of (a) non-hydrogen atoms of guanosine, (b) hydrogen atoms of guanosine, and (c) all atoms of water.

Results

Averaged Structure and B-Factors of Guanosine and Water Molecules. Figure 3 shows the time profile of rmsd from the X-ray structure, including hydrogen atoms. The rmsd was well equilibrated such that the 2 ns MD simulation was long enough for analysis on the average structure and the average fluctuations. The average rmsd for all the atoms from 1 to 2 ns was 0.40 Å, that for all guanosine atoms was 0.36 Å, and that for water was 0.56 Å. Thus, the structure was well conserved. The average kinetic energy, electrostatic potential, Lennard-Jones potential, and internal energy including the energy for 1−4 interactions over the 1−2 ns period were 22.3×10^3, -34.4×10^3, -18.6×10^3, and -34.0×10^3 kcal/mol, respectively. The energy components very rapidly equilibrated within 100 ps. Figure 4 shows the averaged structure of the asymmetric unit calculated for the 1−2 ns period over all asymmetric units in the periodic boundary box. The average displacement of the asymmetric unit coordinates from the X-ray coordinates was 0.154 Å for all atoms, 0.141 Å for all non-hydrogen atoms, and 0.172 Å for all hydrogen atoms, as shown in Figure 5. The non-hydrogen guanosine atoms exhibiting displacements of >0.2 Å were C6 and O6 of GA and GB, N7 of GA, and O5′ of GB. The displacements of guanine base atoms can be explained by a small translation and rotation of the base plane. The displacements of the rotating hydrogen atoms, that is, HO5′, H5′, H5″, HO2′, and HO3′ of guanosine and H1 and H2 of water, were often larger than those of other hydrogen atoms. The displacement of O in W2 was the largest among the water atoms, followed by O in W4, while the displacements of O in W1 and W3 were small. The atoms with large experimental *B*-factors tended to display larger displacements.

As the averaged structure of the asymmetric unit includes disorder in space and thermal fluctuations in time, the translational symmetry of the calculated molecular structures is not perfect, as shown in Figure 2. The *B*-factors in Figure 6 were calculated for a period of 1−2 ns. When the length of the averaging period was changed, the continuous drift of atomic positions resulted in artificially different calculated *B*-factors. However, no clear difference in the calculated *B*-factors was observed in the present case, even when the length of the averaging period was decreased to 50 ps, indicating that the fluctuation in the simulation was well equilibrated. The average relative difference between the calculated and experimental *B*-factors, $|B_{cal} - B_{exp}|/B_{exp}$, in Figure 6 is 22.3% for all atoms. There was some correlation between the *B*-factors and the displacements, for example, O6 had a large *B*-factor and a large displacement.

Figure 7 shows the directional components, B_x, B_y, and B_z, of the oxygen atoms of water. The calculated directional components also coincide well with the experimental values, for both water and guanosine.[11] For most atoms of guanosine, B_x was smallest and B_z was largest. Thus, the motion of guanosine molecules was often smaller in the direction of the glycoside bond and largest in the direction of the columns of stacked guanine bases. B_z was significantly larger than both B_x

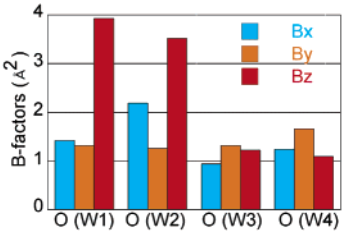

Figure 7. Directional components of the *B*-factors of non-hydrogen atoms of water.

and B_y for the intralayer water molecules W1 and W2, whereas the values of B_x, B_y, and B_z were similar for the interlayer water molecules W3 and W4.

Orientation of Water Molecules. The averaged $\mathbf{v}_b$ and $\mathbf{v}_n$ vectors obtained by simulation were identical to those determined by X-ray analysis, with an averaged rms difference of only 0.04, again demonstrating the high accuracy of the simulated structure. The *z* components of the averaged $\mathbf{v}_b$ vectors were −0.641 (−0.644), −0.559 (−0.761), −0.983 (−0.940), and −0.865 (−0.812) for W1, W2, W3, and W4, respectively, where the numbers in parentheses denote the X-ray values. Thus, $\mathbf{v}_b$ was directed downward in the asymmetric unit with $i_{as} = 0$ and upward in the asymmetric unit with $i_{as} = 1$. The columns of each of these two series of water molecules are energetically favorable structures, with ordered dipole moments. The *y* coordinates of the averaged $\mathbf{v}_n$ for W1 and W3 were 0.976 (0.943) and 0.893 (0.885), respectively, and the *x* coordinate of the averaged $\mathbf{v}_n$ for W4 was 0.900 (0.883). Thus, the $\mathbf{v}_n$ vectors of W1, W3, and W4 were aligned almost parallel to the *xy* plane, consistent with the ordered dipole moments in the *z* direction. However, the *x*, *y*, and *z* coordinates of $\mathbf{v}_n$ for W2 were 0.450 (0.427), 0.473 (0.635), and −0.757 (−0.644), respectively, indicating weaker ordering of the dipole moments of W2.

Although no experimental data have been reported for the order parameter, *S*, of guanosine dihydrate, *S* was easily calculated by the present simulation. The simulated values of *S* for $\mathbf{v}_b$ were 0.771, 0.764, 0.915, and 0.879 for W1, W2, W3, and W4, respectively. Thus, the directions of the dipole moments of the intralayer water fluctuated more than for the interlayer water. The *S* values of $\mathbf{v}_n$ were 0.862, 0.707, 0.907, and 0.809 for W1, W2, W3, and W4, respectively. The difference in *S* of $\mathbf{v}_n$ between the intralayer and interlayer water molecules was not as clear as that for $\mathbf{v}_b$ because $\mathbf{v}_n$ is often affected by switching of hydrogen bonding, rendering it more sensitive to local atomic environments than $\mathbf{v}_b$. The order parameters of $\mathbf{v}_b$ and $\mathbf{v}_n$ were larger for W1 than for W2 and larger for W3 than for W4. The self-correlation functions, $\langle \mathbf{v}_b(t)\cdot\mathbf{v}_b(t+\Delta t)\rangle$ and $\langle |\mathbf{v}_n(t)\cdot\mathbf{v}_n(t+\Delta t)|\rangle$, rapidly converged to approximately $\langle \cos^2\theta\rangle$, which is equivalent to *S*, with a relaxation time of ∼0.05 ps. When $\langle \mathbf{v}_n(t)\cdot\mathbf{v}_n(t+\Delta t)\rangle$ was calculated instead of $\langle |\mathbf{v}_n(t)\cdot\mathbf{v}_n(t+\Delta t)|\rangle$, the functions slowly decreased to zero due to the replacement of H1 and H2. The relaxation times of $\langle \mathbf{v}_n(t)\cdot\mathbf{v}_n(t+\Delta t)\rangle$ for W1, W2, W3, and W4 were approximately 0.1, 0.01, 0.7, and 0.03 ns, respectively. Thus, the replacement of H1 and H2 occurred very slowly, whereas $\mathbf{v}_b$ and $\mathbf{v}_n$ fluctuated rapidly around the average. The replacement of H1 and H2 was significantly slower for W3.

Dynamic Aspects of Hydrogen Bonding of Water Molecules. Figure 8 shows the time profile of hydrogen-bonding probability, P_{hb}, for the four water molecules. Hydrogen bonds with a P_{hb} value smaller than 3% at 2 ns were omitted. All the hydrogen bonds of water with nitrogen atoms of guanosine had P_{hb} values smaller than 3% at 2 ns such that all the hydrogen bonds shown in Figure 8 are concerned with oxygen atoms. All hydrogen bonds that satisfied the hydrogen-bonding criterion in the X-ray structure were included. The water molecules were assumed to be in the (0, 0, 0, 0) asymmetric unit. For example, H1−(O2′, GA, 1, 1, −1, 0) in Figure 8 (W2) denotes the hydrogen bond between (H1, W2, 0, 0, 0, 0) and (O2′, GA, 1, 1, −1, 0). Table 1 shows the geometry of hydrogen bonding in the X-ray structure and the values of P_{hb} at 2 ns.

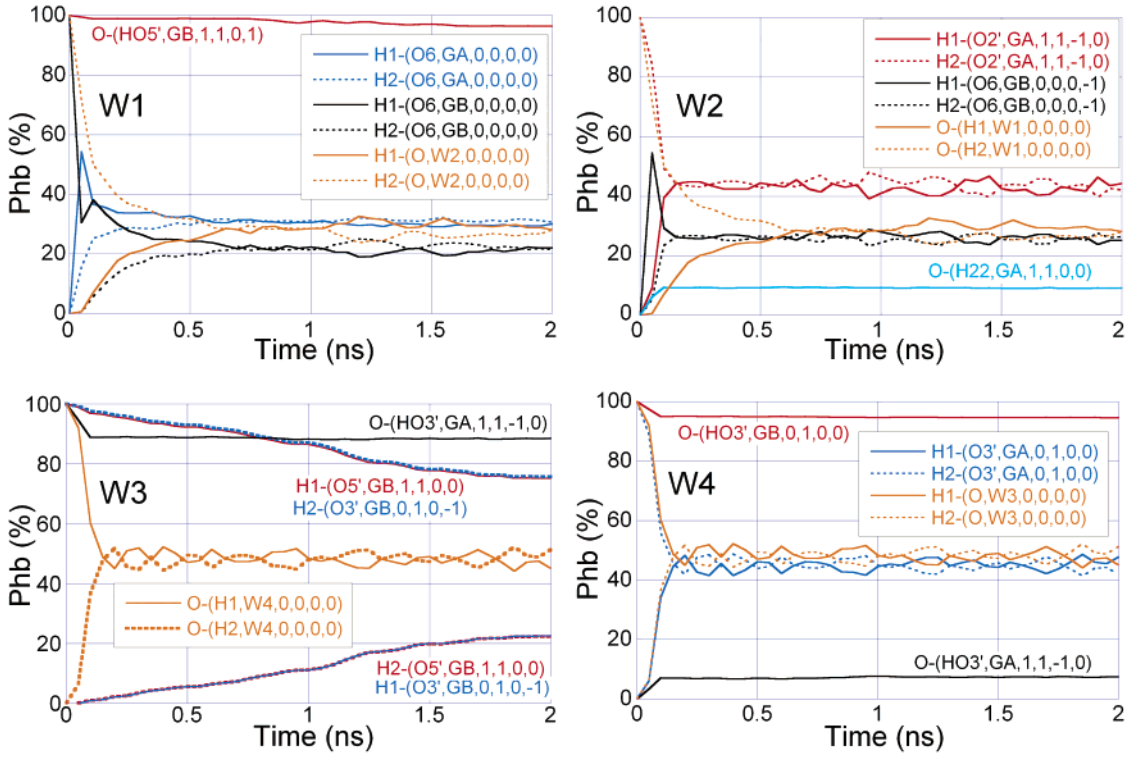

Figure 8. Time profile of hydrogen-bonding probability, P_{hb}.

TABLE 1: Hydrogen Bonding of Water According to the X-ray Structure of Guanosine Crystal

water	hydrogen bond	donor−acceptor distance (Å)	angle of hydrogen−donor−acceptor (deg)	P_{hb} at 2 ns[a] (%)
W1	O−(HO5′, GB, 1, 1, 0, 1)	2.72	9.3	97
	H1−(O6, GB, 0, 0, 0, 0)	2.92	24.2	43
	H2−(O, W2, 0, 0, 0, 0)	2.98	3.7	56
	H1−(O6, GA, 0, 0, 0, 0)[b]	2.93	47.3	61
W2	H2−(O2′, GA, 1, 1, −1, 0)	2.76	15.4	86
	O−(H2, W1, 0, 0, 0, 0)	2.98	3.7	56
	H1−(O6, GA, 0, 0, 0, −1)[b]	3.29	19.3	52
	O−(H22, GA, 1, 1, 0, 0)[b]	2.85	68.2	9
W3	H1−(O5′, GB, 1, 1, 0, 0)	2.75	7.8	98
	O−(H1, W4, 0, 0, 0, 0)	2.78	7.6	96
	H2−(O3′, GB, 0, 1, 0, −1)	2.82	6.9	98
	O−(HO3′, GA, 1, 1, −1, 0)	2.89	8.6	89
W4	O−(HO3′, GB, 0, 1, 0, 0)	2.70	10.0	95
	H1−(O, W3, 0, 0, 0, 0)	2.78	7.6	96
	H2−(O3′, GA, 0, 1, 0, 0)	2.83	2.7	90
	O−(HO3′, GA, 1, 1, −1, 0)[b]	3.5	46.6	7

[a] Values of P_{hb} for H1 and H2 are added. [b] The present hydrogen-bonding criterion is not satisfied in the X-ray structure, but P_{hb} at 2 ns is larger than 5%.

W1 forms seven hydrogen bonds, as shown in Figure 8 (W1). The strongest bond is O−(HO5′, GB, 1, 1, 0, 1), with a P_{hb} value of almost 100%, stably fixing the oxygen atom of W1. Concerning the other six hydrogen bonds, W1 plays the role of a donor, restricting the orientation of W1. When H1 and H2 are not distinguished, some of the hydrogen bonds, such as H1−(O6, GA, 0, 0, 0, 0) and H2−(O6, GA, 0, 0, 0, 0) in Figure 8 (W1), should be considered to form a group. The number of groups of hydrogen bonds of W1 is four. The P_{hb} curves of these bonds oscillate (Figure 8 (W1)), maintaining a constant sum. The oscillation represents the concerted replacement of H1 and H2 by the collective rotation of the water molecules. Similar oscillations are observed for other molecules in Figure 8. The periods of the oscillations are of the order of a few hundred picoseconds. The P_{hb} values of H1 and H2 gradually converge to equal values, and the relaxation time of the convergence is approximately equal to that of the self-correlation function, $\langle \mathbf{v}_n(t)\cdot\mathbf{v}_n(t+\Delta t)\rangle$. In the X-ray structure, (O6, GA, 0, 0, 0, 0) and (O6, GB, 0, 0, 0, 0) are bridged by a hydrogen atom of W1 in the form of a bifurcated hydrogen bond, as shown in Figure 4. In the MD simulation, the same bifurcated hydrogen-bond bridges also appeared frequently, as indicated by the blue circles in Figure 9a. However, (W1, 1, 1, 3, 0) in Figure 9a did not form such a bifurcated hydrogen-bond bridge, instead using both H1 and H2 atoms to bridge the O6 atoms of GA and GB. This two-hydrogen-atom bridge also occurred frequently in the MD animation. Thus, the large fluctuation of the position of W1 in both experimental data and the simulation is due to the coexistence of two types of hydrogen-bond bridges. The two-hydrogen-atom bridge breaks down the hydrogen bond between W1 and W2, yielding a comparatively small P_{hb} value for H2−(O, W2, 0, 0, 0, 0), as shown in Table 1.

Figure 8 (W2) shows the seven hydrogen bonds of W2. When H1 and H2 are not distinguished, the number of groups of hydrogen bonds of W2 is four. The P_{hb} values for the hydrogen bonds with (O2′, GA, 1, 1, −1, 0), (O6, GB, 0, 0, 0, −1), (W1, 0, 0, 0, 0), and (H22, GA, 1, 1, 0, 0) are 86, 52, 56, and 9% at 2 ns, respectively, adding the P_{hb} values for both H1 and H2. The hydrogen-bonding criterion was not satisfied for the hydrogen bond with (H22, GA, 1, 1, 0, 0) in the X-ray structure, as shown in Table 1. As W2 was hydrogen bonded to the ribose atom (O2′, GA, 1, 1, −1, 0) as a donor, an edge of W2 was anchored at the ribose atom.

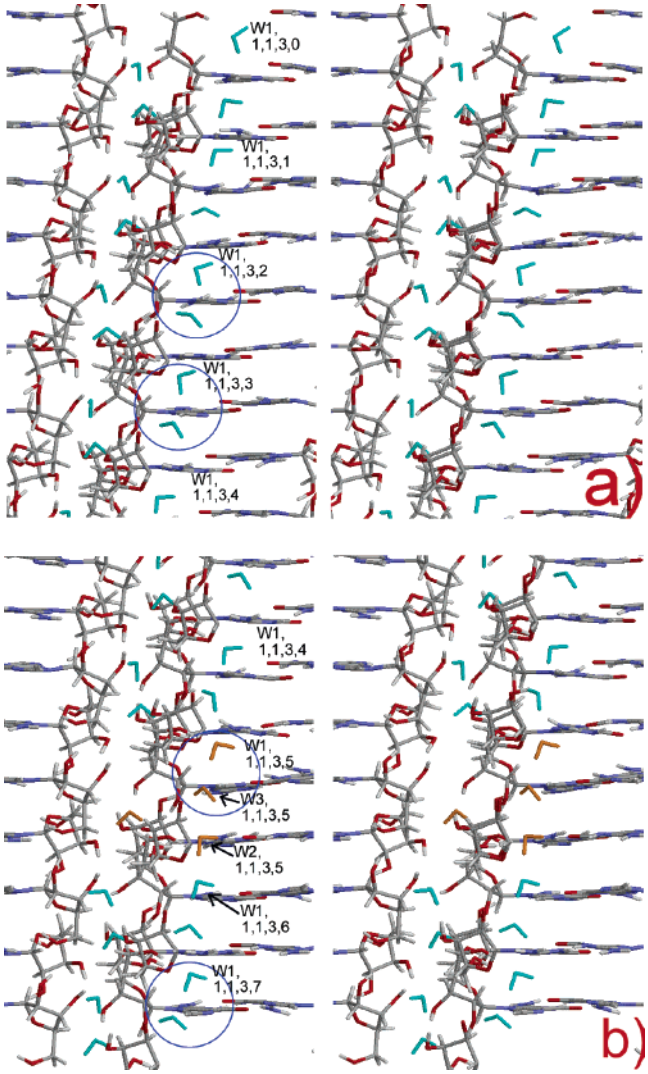

Figure 9. Snapshot of the region around water molecules at 0.777 ns, showing water molecules with $i_{as} = 1$, $i_x = 1$, and $i_y = 3$, with (a) $i_z = 0-3$ and (b) $i_z = 4-7$.[20]

As shown in Figure 8 (W3), W3 formed seven strong hydrogen bonds. When H1 and H2 are not distinguished, the number of groups of hydrogen bonds of W3 is four. The curves of H1−(O5′, GB, 1, 1, 0, 0) and H2−(O3′, GB, 0, 1, 0, −1) were very similar, indicating that (O5′, GB, 1, 1, 0, 0) and (O3′, GB, 0, 1, 0, −1) were a pair of acceptor sites in which water molecules could form hydrogen bonds simultaneously. With replacement of H1 and H2, the curves of H1−(O5′, GB, 1, 1, 0, 0) and H2−(O3′, GB, 0, 1, 0, −1) decreased, whereas those of H2−(O5′, GB, 1, 1, 0, 0) and H1−(O3′, GB, 0, 1, 0, −1) increased. The relaxation time of this replacement of W3 was 3 ns, much longer than that of other water molecules.

W4 formed six hydrogen bonds including one very weak bond, O−(H3′, GA, 1, 1, −1, 0), as shown in Figure 8 (W4). W4 forms a strong bridge between (O3′, GB, 0, 1, 0, 0) and (O3′, GA, 0, 1, 0, 0). When H1 and H2 are not distinguished, the number of groups of hydrogen bonds of W4 is four as well as all other water molecules. As shown in Table 1, the number of groups of hydrogen bonds whose sum of P_{hb} values for H1 and H2 is larger than 80% is one, one, four, and three for W1, W2, W3, and W4, respectively. Thus, the hydrogen bonds of the intralayer water molecules with environments are weaker

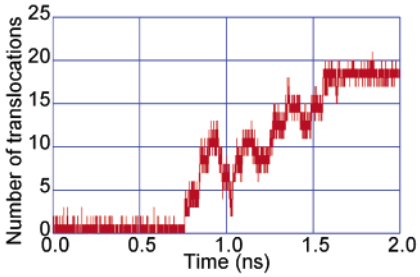

Figure 10. Number of translocated water molecules.

than those of the interlayer water molecules. The hydrogen bonds of W4 were weaker than those of W3, while the hydrogen bond between W3 and W4 was very strong. Thus, the strength of hydrogen bonding of water molecules appears to be closely related to the degree of fluctuation.

Translocation of Water Molecules. Figure 10 shows the time profile of the total number of translocated water molecules. The number increased as the simulation proceeded, representing the accumulation of displacement from the initial X-ray sites. The larger peaks and dips with periods of a few hundred picoseconds represent the concerted translocation of water molecules and their collective return. Most of the translocations were transient, with water molecules rapidly returning to the initial site. Stable translocations were formed in a hesitant manner preceded by many transient movements. Even after the formation of a stable translocation, water molecules often transiently moved back toward the initial site. The short fluctuations in Figure 10 are therefore due to the formation and destruction of these transient translocations.

Using an R_e value of 2.2 Å, doubly occupied sites occurred much more often than empty sites. All 1280 sites in the periodic boundary box were doubly occupied more than once during the 2 ns simulation, whereas only 293 sites became empty. The probability of a site being doubly occupied during the 2 ns simulation was 0.6, 2.9, 0.6, and 0.7% for S1, S2, S3, and S4, respectively. Only six sites were triply occupied more than once, and there were no quadruply occupied sites. A translocation did not always leave an empty site or result in a doubly occupied site because translocations are determined by the nearest neighboring site to the water molecule, not using the criterion R_e.

At 0.759 ns, a notable translocation of (W4, 1, 1, 3, 5) to (S3, 1, 1, 3, 5) occurred. After this, (S4, 1, 1, 3, 5) remained predominantly empty until the end of the simulation. Figure 11 shows the time profile of the *z* coordinates of the related water oxygen atoms. Translocations are indicated by changes in *z* coordinates, and no movement is indicated by a plateau. At 0.760 ns, (W3, 1, 1, 3, 5) moved into the intralayer water column and became fixed between (W1, 1, 1, 3, 5) and (W2, 1, 1, 3, 5). Thus, as shown in Figure 9b, the cavities of S1 and S2 of (1, 1, 3, 5) were occupied by three water molecules, W1, W2, and W3. At 0.780 ns, (W3, 1, 1, 3, 5) translocated to (S1, 1, 1, 3, 5) and (W1, 1, 1, 3, 5) translocated to (S2, 1, 1, 3, 4). Water became surplus at (S2, 1, 1, 3, 4) such that (W2, 1, 1, 3, 4) translocated to (S1, 1, 1, 3, 4) at 0.785 ns. In this domino mechanism, the cluster undergoing water translocation became elongated. W2 translocated to S1, and W1 translocated to S2 in the neighboring unit cell. Figure 11 shows many short plateaus between (S2, 1, 1, 3, i_z) and (S1, 1, 1, 3, i_z + 1), immediately above (S2, 1, 1, 3, i_z), and immediately below (S1, 1, 1, 3, i_z), with typical features indicated by black, blue, and magenta arrows in the figure, respectively. These short plateaus are less stable sites and were occupied by water molecules as

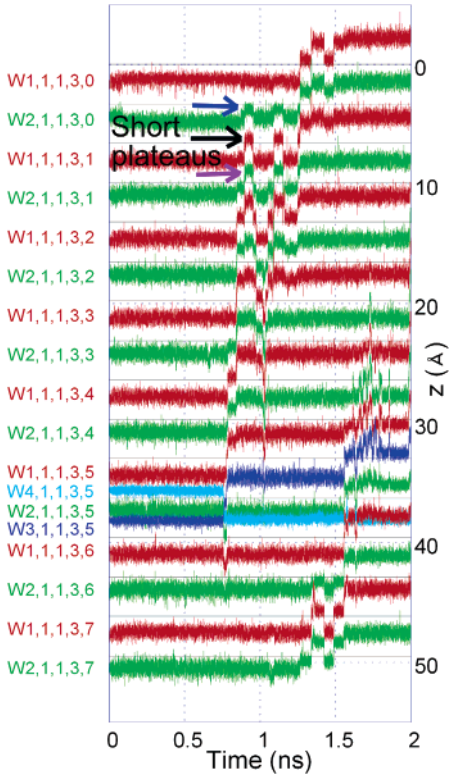

Figure 11. The *z* coordinates of translocated water oxygen atoms. The initial positions of water molecules coincide with water sites.[21]

transition states for the progress of the translocations. The water molecules of this cluster moved in the direction of the dipole moment of water, as shown in Figure 11. At 1.264 ns, (W2, 1, 1, 3, 0) translocated to (S1, 1, 1, 3, 0), and the cluster reached the end of the periodic boundary box. At 1.267 ns, (W1, 1, 1, 3, 0) translocated to (S2, 1, 1, 3, 7), through the periodic boundary. The cluster was further elongated, and (W2, 1, 1, 3, 5) translocated to (S1, 1, 1, 3, 5) at 1.559 ns. Thus, the head of the cluster touched the tail, as shown in Figure 12. The elongation of the cluster continued until the end of the simulation. The translocations at 2 ns were as follows: (W4, 1, 1, 3, 5) → (S3, 1, 1, 3, 5) → (S2, 1, 1, 3, 4) → (S2, 1, 1, 3, 3) → (S2, 1, 1, 3, 2) → (S2, 1, 1, 3, 1) → (S1, 1, 1, 3, 1) → (S2, 1, 1, 3, 0) → (S1, 1, 1, 3, 0) → (S2, 1, 1, 3, 7) → (S1, 1, 1, 3, 7) → (S2, 1, 1, 3, 6) → (S1, 1, 1, 3, 6) → (S2, 1, 1, 3, 5) → (S1, 1, 1, 3, 5) → (S1, 1, 1, 3, 4) → (S1, 1, 1, 3, 3) → (S1, 1, 1, 3, 2). (W2, 1, 1, 3, 4) translocated to (S2, 1, 1, 3, 3) at 2 ns as a result of the accumulation of translocations.

Discussion

The calculation results on the averaged structure from the MD simulation, that is, the averaged geometry, *B*-factors, and orientation vectors of water, were consistent with the known experimental values. Although MD trajectories are always influenced by energy parameters, simulation algorithms, and calculation conditions, the accuracy of the MD simulation performed in a very ordinary style would be satisfactory enough for the present study on the guanosine dihydrate crystal. Thus, we could expect the simulational analysis to be accurate enough also for the dynamical properties that have not been reported experimentally.

The dynamics of the four crystal water molecules in guanosine crystal were analyzed in detail in the present study to further investigate the experimental implications that the structural transition of guanosine crystal is under kinetic or

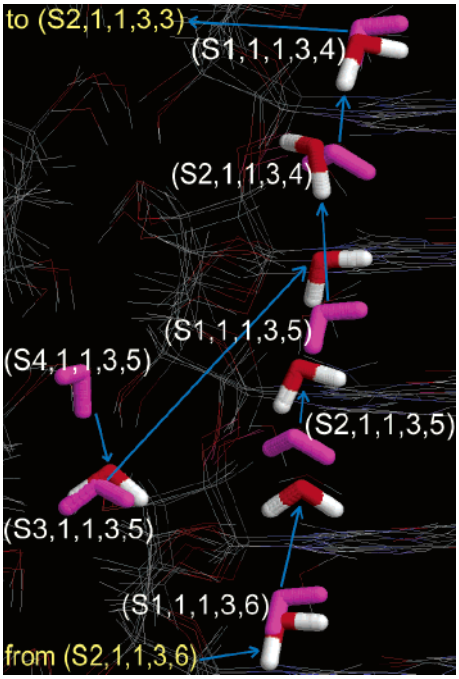

Figure 12. Water structure around (S4, 1, 1, 3, 5) at 1.6 ns. The water molecules are in CPK colors, and the water sites are in magenta.

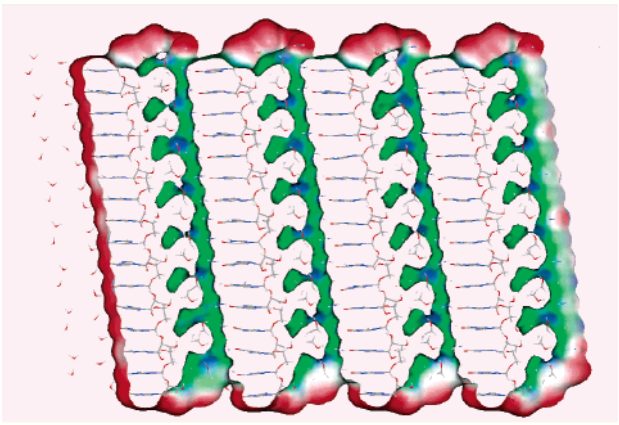

Figure 13. View of the Connolly surface of guanosine molecules at 2 ns, clipped by planes orthogonal to the *y* axis. The green areas denote cavities.

dynamic control. The results indicate that intralayer water molecules move more easily than interlayer water molecules and support the previous hypothesis based on the experimental findings. Structurally, W1 is hydrogen bonded to W2 in the same asymmetric unit, with oxygen atoms separated by 2.98 Å according to the X-ray structure. Although W1 is not hydrogen bonded to W2 of the neighboring asymmetric unit, the distance between that pair of oxygen atoms is also short (i.e., 3.77 Å). Therefore, the cavity containing the W1 and W2 molecules has the form of a column directed in the *c* direction, as shown in Figure 13. The hydrogen-bonding probability, P_{hb}, of W1 with W2 in the same asymmetric unit is ~60% when H1 and H2 are not distinguished (Figure 8), and the hydrogen bond between W1 and W2 of the neighboring asymmetric unit is occasionally formed although the P_{hb} value is <3% in this simulation. Considering this columnar form of the cavity and the ease of movement, it is natural that the columns of intralayer water are the first pathways for the hydration and dehydration of guanosine crystals, while the *a* and *b* directions are resistant to such water migration. The ladder of O6 atoms of GA and GB promotes the translocation of water, supplying a series of equivalent hydrogen-bonding sites.

On the other hand, the cavity formed by interlayer water molecules W3 and W4 is an isolated island structure with long distances between W3 and W4 in the neighboring asymmetric units (i.e., 4.31 Å), although the distance between these two molecules within the same asymmetric unit is short (i.e., 2.78 Å). The islands contain the interlayer water molecules, which are more resistant to translocational movement. However, the islands often become transiently connected with the columns of the intralayer water to form peninsulas as a result of atomic motions, as shown in Figure 13. Interlayer water molecules can then intrude into the intralayer sites via the necks of these peninsulas concerted with the transient hydrogen bond between W3 and W2, as seen for the 0.76 ns translocation. Then, it is suggested that the hydration−dehydration pathway of the water molecules in the island, which has remained obscure experimentally, would be the intralayer columns as is the case of intralayer water molecules.

The mobile water molecules form dynamic hydrogen bonds in the simulation. As shown in Figure 9, the W1 molecule, which forms a bifurcated hydrogen-bond bridge with the two O6 atoms in the X-ray structure, frequently formed another type of bridge using the two hydrogen atoms in the simulation. This two-hydrogen-atom bridge of W1 is not clear in the experimental results but was readily apparent in the simulation. W1 is anchored by the hydrogen bond with HO5′ of GB, and the other hydrogen bonds to multiple surrounding hydrophobic sites are switched. W2 is also anchored by the rigid hydrogen bond with O2′ of GA. Such figures of switching hydrogen bonds of water molecules were reported in the neutron diffraction studies of cyclodextrin hydrates[22,23] and also proposed in the recent neutron diffraction analysis of protein crystals.[24] It is considered to be one of the dynamic figures of water molecules in the first hydration shell around biomolecules.

At 0.76 ns, (W3, 1, 1, 3, 5) was observed to move into the intralayer water column. By this translocation, the water molecules became surplus and less stable in the column, and sequential translocations began. As shown in Figure 11, although the water molecules sometimes retraced their steps, the translocation progressed in the direction of the dipole moment of water over a long period. Thus, the column appears to be a one-way pathway for water flow, acting as a molecular valve mechanism. However, the one-way flow of water was detected only once in the present simulation. Considering that MD simulations produce different atomic trajectories when different initial conditions are provided, much longer and numerous simulations are needed for definite analysis by using a sufficient number of events of water translocations. Therefore, we leave the translocation, the one-way flow, and the molecular valve mechanism as a hypothesis in the present study. Statistical mechanics does not prohibit one-way flow, which may occur when the chemical potential at the two terminals of the pathway is equal. If intralayer water columns are truly one-way pathways, there would be two kinds of columns in the inverse direction in the guanosine crystal due to $P2_1$ symmetry.

Concluding Remarks

The analysis examined directional *B*-factors, orientation vectors, order parameters, the self-correlation function of the orientation vectors, the time profile of hydrogen-bonding probability, the probability of doubly occupied sites, and the formation of large translocation clusters. The differences among the four water sites in each asymmetric unit were shown, with

the primary difference being that intralayer water molecules are more mobile than interlayer water molecules. Columns composed of intralayer water molecules are aligned along the *c* axis and form the easiest pathway for the hydration and dehydration of the guanosine crystal. This pathway would be available for both intralayer water molecules and interlayer water molecules through translocation from the latter to the former. These results support the previous hypothesis based on experimental findings that the phase transition is under kinetic or dynamic control.[7,9] Although much longer and numerous simulations are needed for providing definite insights, we propose a hypothesis that the intralayer water columns should be a one-way pathway for water flow by some molecular valve mechanism, which attracts attention from a viewpoint of water transport across membrane.

Humidity-induced phase transition is not peculiar to guanosine dihydrate. Similar phenomena occur in large numbers of hydrates of biomolecules and drugs.[1,25] For inorganic crystals, MD simulation is frequently used to study the crystal dynamics. On the other hand, in the field of organic crystals, computer simulations have become active in the past decade in the field of polymorphism and ab initio structure determination based on powder diffraction data.[26,27] The results of guanosine dihydrate suggest that MD simulation will be a powerful tool for analyzing individual characters of crystal water molecules in various crystal environments and for considering the mechanisms and dynamics of the phase transition of hydrates.

A characteristic phonon is observed in the low-frequency Raman spectra of nucleosides and nucleotides, and its position shifts in parallel with phase transitions.[7,28] Although the origin of this phonon has not yet been established, it is common to that of the collective mode of nucleic acids in the corresponding region.[28] Analysis of the phonons of guanosine dihydrate based on MD simulations is currently in progress, and the results will be reported elsewhere.

Acknowledgment. This work was partly supported by a Grand-in-Aid for Scientific Research from the Ministry of Education, Culture, Sports, Science and Technology of Japan.

References and Notes

(1) Falk, M. *Can. J. Chem.* **1965**, *43*, 314−318.

(2) Nagashima, N.; Iitaka, Y. *Acta Crystallogr*. **1968**, *B24*, 1136−1138.

(3) Nagashima, N. Doctoral Dissertation, University of Tokyo, Tokyo, Japan, 1985.

(4) Rao, S. T.; Sundaralingam, M. *J. Am. Chem. Soc.* **1969**, *91*, 1210−1217.

(5) Sriram, M.; Liaw, Y.-C.; Gao, Y.-G.; Wang, A. H.-J. *Acta Crystallogr*. **1991**, *C47*, 507−510.

(6) Sugawara, Y.; Kamiya, N.; Iwasaki, H.; Ito, T.; Satow, Y. *J. Am. Chem. Soc.* **1991**, *113*, 5440−5445.

(7) Urabe, H.; Sugawara, Y.; Kasuya, T. *Phys. Rev. B* **1995**, *51*, 5666−5672.

(8) Shindo, Y.; Naito, A.; Tuzi, S.; Sugawara, Y.; Urabe, H.; Saito, H. *J. Mol. Struct.* **2002**, *602*−*603*, 389−397.

(9) Sugawara, Y.; Iimura, Y.; Iwasaki, H.; Urabe, H.; Saito, H. *J. Biomol. Struct. Dyn.* **1994**, *11*, 721−729.

(10) Sugawara, Y.; Nakamura, A.; Iimura, Y.; Kobayashi, K.; Urabe, H. *J. Phys. Chem. B* **2002**, *106*, 10363−10368.

(11) Thewalt, U.; Bugg, C. E.; Marsh, R. E. *Acta Crystallogr.* **1970**, *B26*, 1089−1101.

(12) Case, D. A.; Pearlman, D. A.; Caldwell, J. W.; Cheatham, T. E., III; Ross, W. S.; Simmerling, C. L.; Darden, T. A.; Merz, K. M.; Stanton, R. V.; Cheng, A. L.; Vincent, J. J.; Crowley, M.; Tsui, V.; Radmer, R. J.; Duan, Y.; Pitera, J.; Massova, I.; Seibel, G. L.; Singh, U. C.; Weiner, P. K.; Kollman, P. A. *AMBER 6*; University of California: San Francisco, CA, 1999.

(13) Wang, J.; Cieplak, P.; Kollman, P. A. *J. Comput. Chem*. **2000**, *21*, 1049−1074.

(14) Jorgensen, W. L.; Chandrasekhar, J.; Madura, J. D.; Impey, R. W.; Klein, M. L. *J. Chem. Phys.* **1983**, *79*, 926−935.

(15) Essman, U.; Perera, L.; Berkowitz, M. L.; Darden, T.; Lee, H.; Pedersen, L. G. *J. Chem. Phys.* **1995**, *103*, 8577−8593.

(16) Berendsen, H. J. C.; Postma, J. P. M.; van Gunsteren, W. F.; DiNola, A.; Haak, J. R. *J. Chem. Phys.* **1984**, *81*, 3684−3690.

(17) McCammon, J. A.; Harvey, S. C. *Dynamics of Proteins and Nucleic Acids*; Cambridge University Press: Cambridge, U.K., 1987.

(18) Schindler, H.; Seelig, J. *Biochemistry* **1975**, *14*, 2283−2287.

(19) Markley, J. L.; Bax, A.; Arata, Y.; Hilbers, C. W.; Kaptein, R.; Sykes, B. D.; Wright, P. E.; Wüthrich, K. *Pure Appl. Chem.* **1998**, *70*, 117−142.

(20) Seen along the *y* axis. The *z* direction is downward. Some guanine bases were omitted to avoid overlap. The molecules in yellow are the water molecules of (1, 1, 3, 4) that participate in triggering the formation of the large translocation cluster. The water molecules with no labels can be identified by reference to Figure 1. The blue circles denote the W1 and W2 molecules with orientations similar to those in the X-ray structure.

(21) As the water molecules in Figure 11 are asymmetric units with $i_{as} = 1$, the *z* component of their dipole moments is negative. The thin black horizontal lines denote the *z* coordinates of the O6 atoms of guanine bases in the X-ray structure. Some short plateaus of transient water sites are indicated by arrows.

(22) Saenger, W.; Betzel, Ch.; Hingerty, B.; Brown, G. M. *Nature* **1982**, *296*, 581−583.

(23) Betzel, Ch.; Saenger, W.; Hingerty, B. E.; Brown, G. M. *J. Am. Chem. Soc*. **1984**, *106*, 7545−7557.

(24) Chatake, T.; Ostermann, A.; Kurihara, K.; Parak, F. G.; Niimura, N. *Proteins* **2003**, *50*, 516−523.

(25) Haleblian, J. K. *J. Pharm. Sci*. **1975**, *64*, 1269−1288.

(26) *Theoretical Aspects and Computer Modeling of the Molecular Solid State*; Gavezzotti, A., Ed.; John Wiley and Sons: Chichester, U.K., 1997.

(27) *Molecular Modeling Applications in Crystallization*; Myerson, A. S., Ed.; Cambridge University Press: Cambridge, U.K., 1999.

(28) Urabe, H.; Sugawara, Y.; Tsukakoshi, M.; Kasuya, T. *J. Chem. Phys.* **1991**, *95*, 5519−5523.